

An NAC transcription factor orchestrates multiple features of cell wall development in *Medicago truncatula*

Qiao Zhao¹, Lina Gallego-Giraldo¹, Huanzhong Wang¹, Yining Zeng^{2,3}, Shi-You Ding^{2,3}, Fang Chen^{1,3} and Richard A. Dixon^{1,3,*}

¹Plant Biology Division, Samuel Roberts Noble Foundation, 2510 Sam Noble Parkway, Ardmore, OK 73401, USA,

²Chemical & Biosciences Center, National Renewable Energy Laboratory, 1617 Cole Blvd. Golden, CO 80401, USA, and

³Bioenergy Sciences Center (BESC), Oak Ridge, TN, USA

Received 11 February 2010; revised 23 March 2010; accepted 31 March 2010; published online 5 May 2010.

*For correspondence (fax +1 580 224 6692; e-mail radixon@noble.org).

SUMMARY

To identify genes controlling secondary cell wall biosynthesis in the model legume *Medicago truncatula*, we screened a *Tnt1* retrotransposon insertion mutant population for plants with altered patterns of lignin autofluorescence. From more than 9000 R1 plants screened, four independent lines were identified with a total lack of lignin in the interfascicular region. The mutants also showed loss of lignin in phloem fibers, reduced lignin in vascular elements, failure in anther dehiscence and absence of phenolic autofluorescence in stomatal guard cell walls. Microarray and PCR analyses confirmed that the mutations were caused by the insertion of *Tnt1* in a gene annotated as encoding a NAM (no apical meristem)-like protein (here designated *Medicago truncatula* NAC SECONDARY WALL THICKENING PROMOTING FACTOR 1, MtNST1). MtNST1 is the only family member in *Medicago*, but has three homologs (AtNST1–AtNST3) in *Arabidopsis thaliana*, which function in different combinations to control cell wall composition in stems and anthers. Loss of MtNST1 function resulted in reduced lignin content, associated with reduced expression of most lignin biosynthetic genes, and a smaller reduction in cell wall polysaccharide content, associated with reduced expression of putative cellulose and hemicellulose biosynthetic genes. Acid pre-treatment and cellulase digestion released significantly more sugars from cell walls of *nst1* mutants compared with the wild type. We discuss the implications of these findings for the development of alfalfa (*Medicago sativa*) as a dedicated bioenergy crop.

Keywords: NAC transcription factor, lignification, cell wall development, stomatal guard cell, anther dehiscence, bioenergy.

INTRODUCTION

Plant secondary cell walls constitute the most abundant biomass on earth, and can potentially be utilized for biofuel production via sugar release and fermentation (Somerville, 2007; Carroll and Somerville, 2009). Secondary walls are deposited inside the primary walls after the cells cease expansion (Turner *et al.*, 2001). The ability to produce secondary walls has enabled vascular plants to form strong, thick-walled cells for water transport and mechanical support. Secondary wall thickening plays important roles in various biological processes, such as the formation of tracheary elements and fibers, anther dehiscence, and the shattering of seed pods.

Secondary cell walls are composed mostly of cellulose, lignin and hemicellulose. In recent years, the application of genetic and genomic strategies has led to significant progress in identifying and characterizing the genes involved in the biosynthesis of these cell wall components

(Boerjan *et al.*, 2003; Tanaka *et al.*, 2003; Liepman *et al.*, 2005; Somerville, 2006). Although secondary cell wall components are synthesized at different subcellular locations, the expression of the genes involved is highly coordinated, both temporally and spatially.

Recently, NAC (NAM, ATAF and CUC2) and MYB family transcription factors have been shown to play key roles in regulating secondary wall biosynthesis in *Arabidopsis thaliana* (Mitsuda *et al.*, 2007; Zhong *et al.*, 2007, 2008; Mitsuda and Ohme-Takagi, 2008; Zhou *et al.*, 2009). Two *Arabidopsis* NAC genes, *NAC SECONDARY WALL THICKENING PROMOTING FACTOR 1* (*NST1*) and *NST2*, were shown to function together in the promotion of secondary wall thickening in the anther endothecium, a process that is necessary for anther dehiscence (Mitsuda *et al.*, 2005). In addition, the simultaneous knock-out of *NST1* and another *NST* gene, *NST3*, resulted in the loss of secondary wall

deposition in Arabidopsis stems, whereas single knock-outs in *NST1* or *NST3* show no phenotype (Mitsuda *et al.*, 2007; Mitsuda and Ohme-Takagi, 2008). It was proposed that *NST* genes are master switches, capable of turning on the entire biosynthetic pathways for cellulose, xylan and lignin by initiating a transcriptional signaling network to direct downstream targets, including MYB transcription factors (Zhong *et al.*, 2008).

Barrel medic (*Medicago truncatula*) has been developed as a model legume with extensive genomic and genetic resources (Town, 2006; Benedito *et al.*, 2008; Young and Udvardi, 2009). It is very closely related to alfalfa (*Medicago sativa*), the world's major forage legume, and potentially a dedicated bioenergy crop (Yang *et al.*, 2009). Previous studies on engineering cell walls to improve biomass processing in alfalfa have directly targeted the enzymes of the lignin biosynthetic pathway (Reddy *et al.*, 2005; Chen *et al.*, 2006; Shadle *et al.*, 2007). Here, we describe a non-biased, forward genetic approach to discover genes determining levels and spatial patterns of lignification in *M. truncatula*. Retrotransposon insertions in the *MtNST1* gene result not only in the loss of lignification in the interfascicular region of the stem, and in the prevention of anther dehiscence, but also in alterations in the cell walls of stomatal guard cells. We describe the metabolic and transcriptional changes associated with the loss of *MtNST1* function, and the impacts of *NST1* downregulation on cell wall recalcitrance to saccharification. We also discuss the implications of these studies for the development of alfalfa as a dual forage/bioenergy crop.

RESULTS

Isolation and characterization of *M. truncatula nst1* mutants

To identify mutants with defects in secondary cell wall formation, an R1 population of tobacco *Tnt1* retrotransposon insertion-mutagenized *M. truncatula* (Tadege *et al.*, 2005, 2008) was screened by UV microscopy of cross sections of the sixth stem internodes, where lignification is well developed in wild-type plants. Approximately 3400 independent R1 lines (around 9000 plants) were analyzed, and several lines with significantly altered extents and/or patterns of lignin autofluorescence were observed (Figure S1). One of these lines showed a dramatic loss of lignin in interfascicular fibers (Figure S1b). To better characterize developmental patterns of lignification in this mutant (line NF3056), we compared autofluorescence in cross sections from the second to fifth internodes (from top to bottom) of NF3056 and wild-type R108 *M. truncatula* (Figure 1). In the wild-type plant, lignin starts to accumulate in vascular tissues at an early stage (Figure 1e), and is most intensely located in secondary walls of vascular tissues, pith rays and fibers at late stages (Figure 1h). Compared with the wild-type plant,

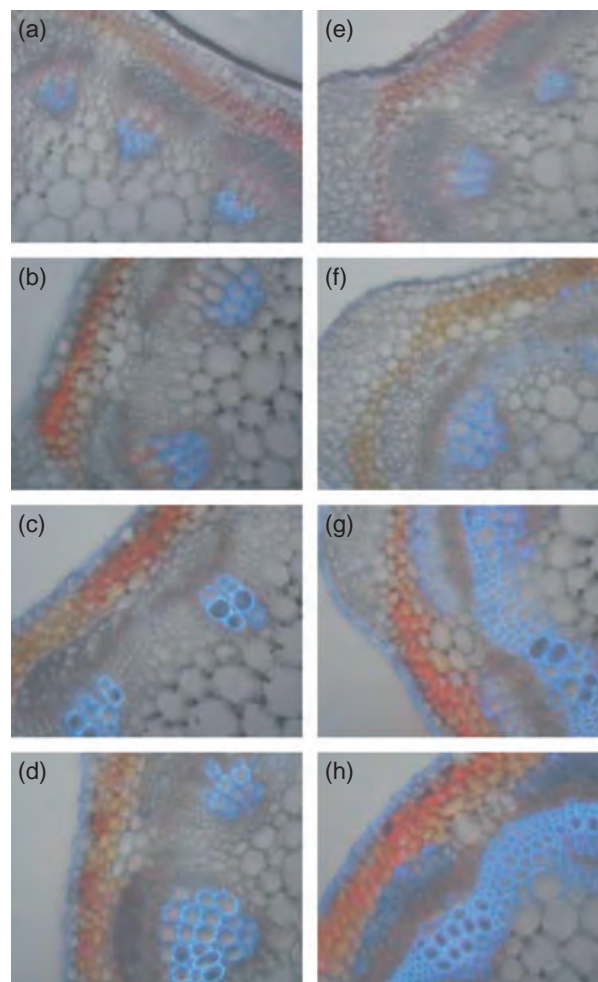


Figure 1. The *nst1-1* line shows defects in lignin deposition in stems. (a–d) Cross sections of stems of 9-week-old *nst1-1* plants taken from the second, third, fourth and fifth internodes, respectively. (e–h) As above, for wild-type *Medicago truncatula*. Total lignin was visualized by UV autofluorescence.

NF3056 shows no difference in the location or intensity of lignin autofluorescence at the early stage (Figure 1a,e), but there was clearly less lignin in the third internode and below, and the lignin was only deposited in vascular cells, in contrast to the strong lignification in the interfascicular region and the phloem fibers in the wild-type (compare Figure 1b–d, f–h). The level of lignin autofluorescence in vascular elements also appeared somewhat lower in mutant compared with wild-type plants. Although lignin fluorescence was absent from phloem fibers in the mutant, the phloem tissues appeared normal under the light microscope (Figure S2).

To identify the gene responsible for the tissue-specific loss of lignification, microarray analysis was performed with RNA isolated from lignifying stem internodes of NF3056. As *Medicago Tnt1* retrotransposon lines generally contain 20–50 insertions (Tadege *et al.*, 2008), progeny from the

same parent plant segregating with the wild-type lignification phenotype were used as controls. Total RNA samples from triplicate biological replicates of the mutants and controls were subjected to Affymetrix microarray analysis. In total, 152 probe sets were downregulated in the mutant line by at least twofold (Table S1). To identify the gene with the *Tnt1* retrotransposon insertion, PCR was performed with a *Tnt1* primer and primers designed from the probe set sequences: this was done sequentially in order of the extent of downregulation of the 152 probe sets. PCR amplification using primers complementary to the three most downregulated genes in Table S1, each of which is annotated as encoding a gene involved in cell wall biosynthesis, did not lead to amplification of a PCR product, whereas the fourth candidate (Mtr.33913.1.S1_at, expression level decreased by 22-fold) was confirmed to contain a *Tnt1* retrotransposon insert. The probe set Mtr.33913.1.S1_at is annotated as representing a NAM (no apical meristem)-like protein.

Using the Mtr.33913.1.S1_at probe sequence, a cDNA BLAST search was performed against the *M. truncatula* genome from the Dana-Faber Cancer Institute (DFCI) bioinformatics web site (<http://compbio.dfci.harvard.edu/tgi/cgi-bin/tgi/gimain.pl?gudb=medicago>). The first hit with the lowest e-value was TC141793, which contains a 1113-bp

cDNA sequence, including the entire Mtr.33913.1.S1_at probe sequence. Using the TC141793 sequence, a nucleotide BLAST search was then performed against the NCBI database, and the first hit was Arabidopsis *NST1* (At2g46770), a recently discovered NAC transcription factor responsible for secondary wall thickening (Mitsuda *et al.*, 2005; Zhong *et al.*, 2007). As TC141793 does not contain the full-length cDNA, 3'-RACE was performed to complete the cDNA sequence. Because NF3056 phenocopies the Arabidopsis *nst1:nst3* double mutant, and TC141793 shares sequence similarity with Arabidopsis *NST1*, we named the full-length sequence *MtNST1* (GenBank accession number GU144511), and the NF3056 mutant *nst1-1*.

Protein sequence alignment was performed using the deduced amino acid sequence of *MtNST1*, and Arabidopsis *NST1*, *NST2* and *NST3*. Because Arabidopsis *NST1* and *NST2* are more similar to each other than either is to *NST3*, we first aligned *MtNST1* with *AtNST1* and *NST2* (Figure 2a), and then aligned the *Medicago* sequence separately with *AtNST3* (Figure S3). *MtNST1* shares high sequence similarity with all three *AtNST* proteins at the conserved N-terminal NAC domain. The level of conservation is comparable with that between *AtNST* proteins. However, the C-terminal domain of *MtNST1* is quite distinct, indicating that *MtNST1*

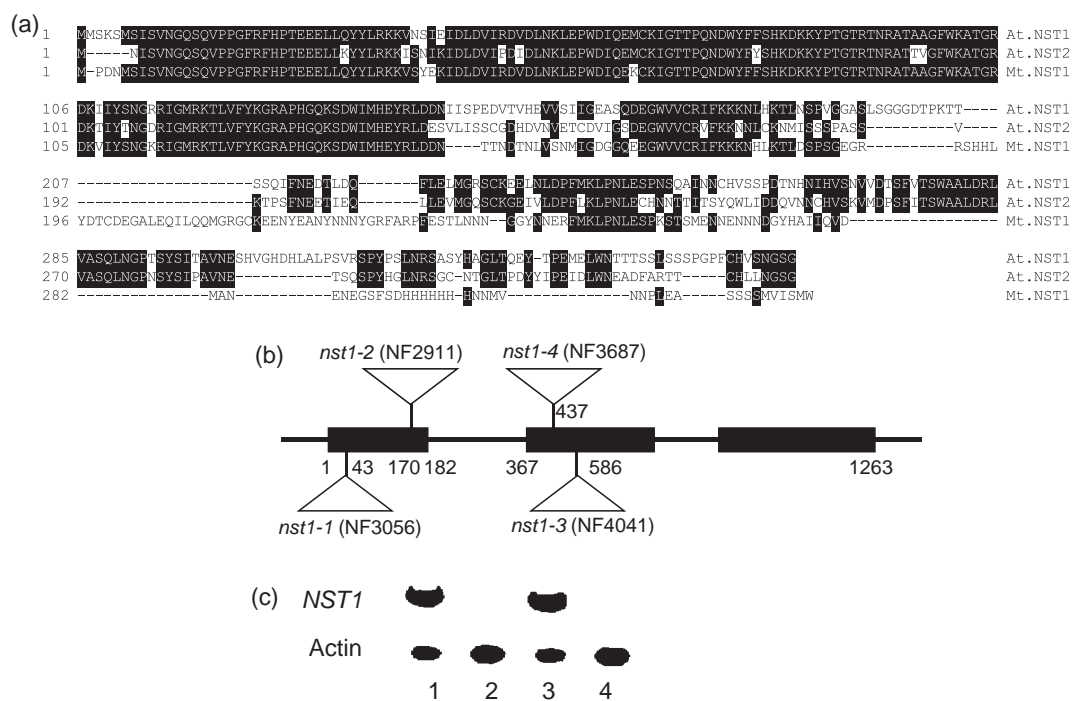


Figure 2. Characterization of *MtNST1*.

(a) Amino acid sequence alignments of Arabidopsis *AtNST1*, *AtNST2* and *AtNST3* with the deduced *Medicago truncatula* *MtNST1*. Black shading indicates identical amino acids.

(b) Schematic diagram of the structure of the *MtNST1* gene and the positions of *Tnt1* retrotransposon insertions in the *nst1-1* (NF3056), *nst1-2* (NF2911), *nst1-3* (NF4041) and *nst1-4* (NF3687) lines. Numbers indicate nucleotide positions from the site of initiation of translation. Boxes represent exons.

(c) RT-PCR analysis of *MtNST1* transcripts in wild-type and *Tnt1* insertion lines. Actin was used as a loading control. Lanes 1 and 3 are wild type; lanes 2 and 4 are *nst1-1* and *nst1-2*, respectively.

might have different functional characteristics. The overall sequence similarity between MtNST1 and AtNST proteins is only around 50%, even though the NAC domain is highly conserved.

Because of the problem of remobilization of *Tnt1* elements during tissue culture (Tadege *et al.*, 2005), we did not attempt to directly complement *nst1-1* with the *MtNST1* open reading frame. Instead, to confirm that the tissue-specific loss-of-lignification phenotype was indeed the result of insertional mutagenesis of *MtNST1*, we obtained three further independent alleles. The first (NF2911) was obtained by forward genetic screening as above, on the basis of the loss of interfascicular fluorescence, and micro-array analysis confirmed the downregulation of many, but not all, of the genes shown to be downregulated in *Mtnst1*, including the *NST1* gene itself (Table S1). PCR analysis then confirmed the insertion of a *Tnt1* transposon in *MtNST1*. We then used *MtNST1* gene-specific primers for the reverse genetic screening of DNA pools from the complete *Tnt1* mutant population. Two additional independent lines (NF4041 and NF3687) were positive for the presence of *Tnt1* insertions in *MtNST1*, and homozygous lines of both showed the altered lignification phenotype (Figure S4). *Tnt1* flanking sequence analyses indicated that *Tnt1* is inserted in the *NST1* gene in the first exon, at 43 (*nst1-1*, NF3056) or 170 bp (*nst1-2*, NF2911), or in the second exon at 586 (*nst1-3*, NF4041) or 437 bp (*nst1-4*, NF3687) (Figure 2b). RT-PCR analysis confirmed that no *MtNST1* transcript was present in any of the four mutant lines (Figure 2c and S4e).

As a final validation that the loss of lignin phenotype is caused by a loss of function of *MtNST1*, we obtained another line, by forward genetic screening, harboring a point mutation rather than a transposon insertion in *MtNST1* (H. Wang, R.A. Dixon and F. Chen, unpublished data). Plants heterozygous for both the point mutation allele and the *Tnt1* insertion allele at the *MtNST1* locus showed loss of interfascicular lignification, further confirming *NST1* as the gene controlling the lignification phenotype.

Cell wall composition of *Mtnst1* mutant stems

The total lignin content of stem internodes 5–8, as determined by the acetyl bromide method (Fukushima and Hatfield, 2004), was reduced by around 50% in the *Mtnst1* mutant compared with wild-type plants (Figure 3a). Thioacidolysis (Lapierre *et al.*, 1985) revealed a reduction in G lignin levels in stems of *Mtnst1* mutants, but a proportionately larger decrease in S lignin, such that the S/G ratio was dramatically reduced in the mutants (Figure S5).

The same cell wall samples used for lignin analysis were analyzed for total sugar content by phenol-sulfuric assay (Dubois *et al.*, 1956). Total sugar levels were somewhat reduced in *nst1* mutants compared with wild-type plants (Figure 3b). Analysis of monosaccharide composition indicated that glucose, xylose, galactose and arabinose were the

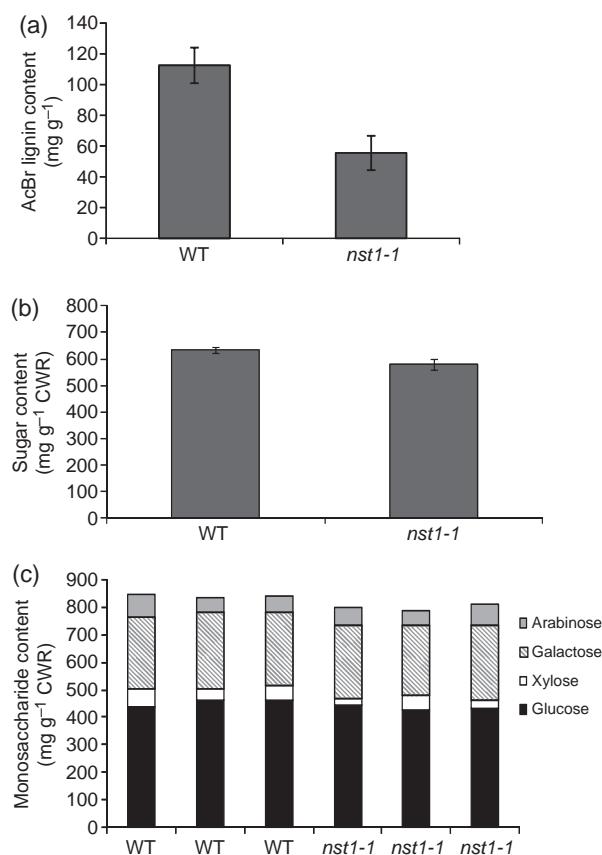


Figure 3. Cell wall composition of wild type and *nst1-1*.

(a) Acetyl bromide lignin content of the stems (internodes 5–8); $n = 10$.

(b) Total sugar content of cell walls from stems of the wild type and *nst1-1*; $n = 6$.

(c) Monosaccharide composition of stems (internodes 5–8) from the wild type and *nst1-1* (biological triplicates).

Data are means of duplicate assays; CWR, cell wall residue; the bars are means and SDs for 10 (a) or six (b) biological replicates.

major sugar components of the *M. truncatula* cell wall, with galactose levels being significantly higher than in Arabidopsis (Zhong *et al.*, 2008) (Figure 3c). In comparison with the wild type, cell walls from *nst1* mutants had slightly decreased levels of glucose and xylose, whereas there was no significant change in galactose or arabinose levels (Figure 3c). In contrast, Arabidopsis plants with a loss of NST function through expression of a chimeric NST repressor exhibit significantly reduced levels of xylose, and nearly double the levels of galactose and arabinose, compared with controls (Iwase *et al.*, 2009). The change in overall monosaccharide composition in the *Mtnst1* mutants is likely to stem from a reduced deposition of cellulose and hemicellulose in the defective secondary walls of the interfascicular fiber cells.

Levels of wall-bound phenolic compounds were determined by HPLC analysis of alkaline hydrolysates of cell wall material. The stem cell walls contained low levels of alkali-releasable vanillin, *p*-coumaric and ferulic acids. Apart from

a small reduction in vanillin, the loss of function of *Mtnst1* had little effect on wall-bound phenolic levels (Figure S6).

Soluble phenolic compounds in *M. truncatula nst1* mutants

HPLC analysis was used to compare the profiles of soluble phenolic compounds in wild-type and mutant plants. The major soluble phenolics in *Medicago* stems are a series of glycosides of the flavones apigenin and luteolin (Kowalska et al., 2007). Pairwise comparisons of the *nst1-1* and *nst1-2* lines with corresponding controls indicated no clear quantitative or qualitative differences in soluble phenolic profiles (Figure S7).

Growth characteristics of *M. truncatula nst1* mutants

At first sight, the overall growth phenotypes of the four independent *nst1* mutant lines appeared similar to those of wild-type plants, although the branches were less able to support themselves against gravity, presumably because of the defect in secondary wall formation (Figure S8a). Vegetative growth was not strongly affected in the *Mt-nst1* mutant lines, but stem length was reduced by around 25%, and the average leaf area increased by around 14% (Figure S8b; Table 1). The reduction in stem length was mainly the result of a reduction of internode length in the three most mature internodes at the 12-internode stage (Figure S9). Flowering time and stem diameter were not affected in the mutant lines (Table 1).

Stomatal phenotype of *Mtnst1* mutants

Examination of leaf epidermal cells revealed a significant loss of fluorescence signal in stomatal guard cells of homozygous mutant leaves, compared with the wild type (Figures 4a,b and S10). This was observed in all four independent *nst1* alleles. Furthermore, after a light induction period, the guard cells of the *nst1* mutant exhibited a striking reduction in stomatal aperture, of around 80% compared with controls (Figure 4c,d; Table 2). This was associated with a reduction in transpiration rate in the *nst1* mutants,

accompanied by a small but significant increase in the photosynthetic rate (Table 2).

The autofluorescence of stomatal guard cells has been proposed to result from the presence of wall-associated pectin-linked ferulic acid (Jones et al., 2005). To determine whether NST1 knock-out lines exhibited reduced wall-bound ferulic acid levels in leaf tissues, we first measured the total wall-bound phenolic levels in leaf panels (minus veins). Levels of coumaric, caffeic and ferulic acids were similar in extracts from the wild type and mutant lines. However, although the data suggested small increases in wall-bound coumaric and caffeic acid levels, and a small (less than 10%) reduction in wall-bound ferulic acid levels, these apparent changes were not statistically significant (data not shown).

To better address changes in phenolic compounds in the guard cells of *Mtnst1* mutants, we used Coherent anti-Stokes Raman spectroscopy (CARS) (Zeng et al., 2010) to directly visualize ferulate signals in the walls. Previous Raman spectroscopy studies have demonstrated the capability of detecting ferulate by using specific Raman bands (Ram et al., 2003; Hélène et al., 2008). The sharp Raman band at 1600 cm⁻¹ corresponds to the stretch vibration of the aromatic ring structure in ferulate. Similar to ordinary spontaneous Raman scattering, CARS offers chemical contrast based on the intrinsic Raman vibrational frequencies of the molecules of interest in the sample. However, because of the coherent nature, CARS offers orders of magnitude higher sensitivity than spontaneous Raman. The stomatal guard cells, and the central cavity between the cells of the complex, showed a bright CARS signal caused by the presence of ferulate in the epidermal peels of leaves of wild-type plants (Figure 4e,f). In contrast, this signal was largely absent on analysis of mutant plants (Figure 4g,h).

Anther dehiscence in *Mtnst1* mutants

Arabidopsis NST1 and NST2 together regulate secondary wall thickening in the anther endothecium, and *nst1:nst2* double mutants show a defect in anther dehiscence

Line	Stem height (cm)	Flowering node	Mean internode length (cm)	Leaf area (mm ²)	Stem diameter (mm)
Wt1	70.4 ± 0.5	11.5 ± 0.6	5.9 ± 0.5	5.0 ± 0.2	1.6 ± 0.2
<i>nst1-1</i>	60.8 ± 0.6	11.0 ± 0.3	5.1 ± 0.2	6.4 ± 0.3	1.6 ± 0.1
Wt2	67.7 ± 0.7	10.8 ± 0.6	5.7 ± 0.5	9.1 ± 0.5	2.0 ± 0.2
<i>nst1-2</i>	65.0 ± 0.6	12.0 ± 0.8	5.4 ± 0.4	11.0 ± 0.8	1.9 ± 0.3
Wt3	70.3 ± 0.4	11.5 ± 0.6	5.9 ± 0.3	6.2 ± 0.4	1.6 ± 0.1
<i>nst1-3</i>	61.5 ± 0.4	11.0 ± 0.7	5.1 ± 0.3	7.3 ± 0.8	1.8 ± 0.2
^a Average					
Wt	69.5 ± 0.3	11.2 ± 0.5	5.8 ± 0.2	6.9 ± 0.6	1.73 ± 0.1
<i>nst1</i>	62.4 ± 0.4	11.3 ± 0.6	5.2 ± 0.3	8.1 ± 0.7	1.76 ± 0.2

Table 1 Growth parameters of independent *nst1* insertion mutants

Results are the means of six stems per line ± SE. For each mutant line analyzed, a wild-type (Wt) was grown in parallel.

^aAverage of the combined data for Wt1, 2 and 3 and *nst1-1*, -2 and -3.

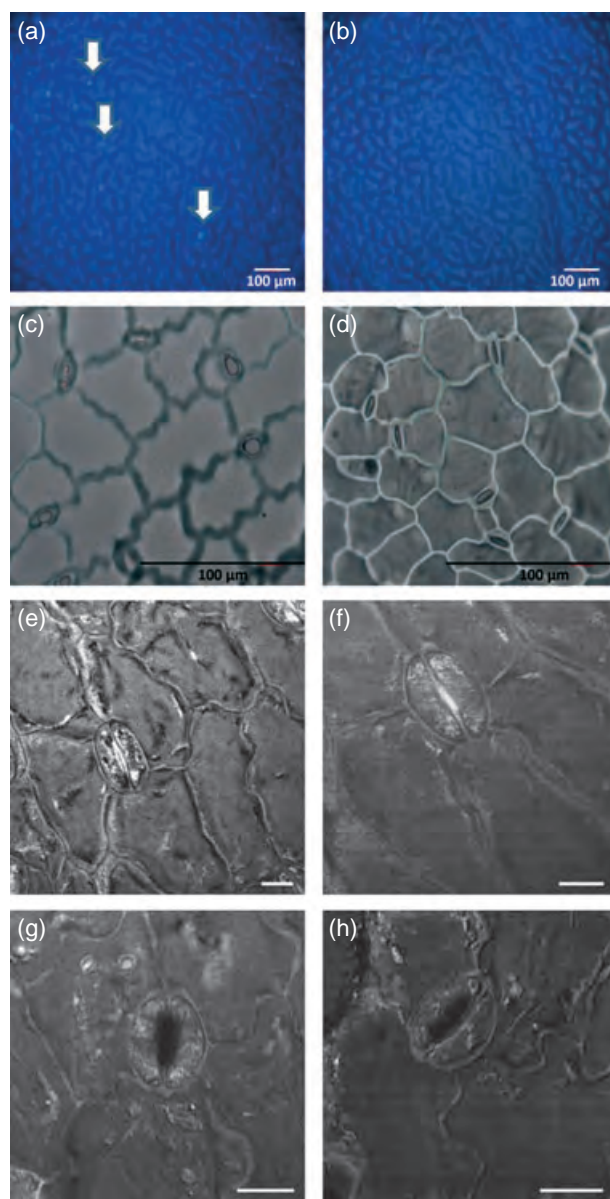


Figure 4. Stomatal phenotypes of *nst1* mutants.

(a, b) Representative picture of leaf epidermal cells in (a) control and (b) the *Mtnst1* mutant. The light-blue autofluorescence signal (typical signals marked by white arrows) comes from stomatal guard cells.

(c, d) Picture showing differences in stomatal aperture after 2 h of light induction in (c) control and (d) the *Mtnst1* mutant.

(e–h) Coherent anti-Stokes Raman spectroscopy (CARS) microscopy of epidermal strips from (e, f) the wild type and (g, h) *Mtnst1* mutant plants. The bright signals in the stomatal complexes of wild-type plants are the Raman bands at 1600 cm^{-1} originating from ferulate.

(Mitsuda *et al.*, 2005). Flowers of all four independent *Mtnst1* mutants had indehiscent anthers, whereas the pollen grains are released normally from wild-type anthers (Figures 5a,b and S11). To examine pollen viability in the *nst1* flowers, Alexander's staining method was used (Alexander, 1969). Light microscopy showed that the pollen grains from

Table 2 Stomatal aperture, transpiration rate and photosynthetic rate of independent *nst1* insertion mutants

Line	Photosynthetic rate ($\mu\text{mol CO}_2\text{ m}^{-2}\text{ sec}^{-1}$)	Transpiration rate ($\text{mmol H}_2\text{O m}^{-2}\text{ sec}^{-1}$)	Stomatal aperture
Wt1	13.1 ± 0.2	4.5 ± 0.1	1.5 ± 0.3
<i>nst1-1</i>	14.2 ± 0.3	3.9 ± 0.2	3.6 ± 0.3
Wt2	14.2 ± 0.1	4.1 ± 0.2	1.7 ± 0.2
<i>nst1-2</i>	15.8 ± 0.2	3.5 ± 0.2	4.6 ± 0.3
Wt3	14.2 ± 0.3	4.3 ± 0.1	1.8 ± 0.2
<i>nst1-3</i>	15.3 ± 0.1	3.6 ± 0.1	5.2 ± 0.3
^a Average			
Wt	13.8 ± 0.2	4.3 ± 0.1	1.6 ± 0.2
<i>nst1/nst1-nst3</i>	15.1 ± 0.2	3.6 ± 0.2	4.5 ± 0.3

Photosynthetic and transpiration rates are the means of six values (three replicates taken on two different days) \pm SE. The stomatal aperture data (ratio between lengths and widths) are the means of 75 stomatal guard cells distributed in three different areas of the film strips \pm SE. For each mutant line analyzed, a wild-type (Wt) was grown in parallel.

^aAverage of the combined data for Wt1, 2 and 3 and *nst1-1*, -2 and -3.

Mtnst1-1 take up the stain, and are therefore viable; they also exhibit normal shape and size (Figure 5c,d). *M. truncatula* is a self-pollinating species: as a result of the impairment of anther dehiscence, mature plants of the *nst1* mutants generally failed to develop seed pods, although a few very small pods were occasionally observed on old plants.

Potential downstream target genes for *MtNST1* action

Because of the existence of multiple *Tnt1* insertions in the *Medicago* mutant lines, the initial microarray analysis by which the *NST1* gene was identified does not provide a definitive indication of co-regulated or potential downstream target genes for *NST1* action. We therefore performed a parallel gene expression analysis using RNA from stems of an independent allele. Of the 152 probe sets that were downregulated by more than twofold in the *nst1-1* mutant compared with its null segregant control, 94 were also downregulated by more than twofold in the *nst1-2* mutant, compared with its null segregant control. Eighteen probe sets were also upregulated by more than twofold in both mutant lines (Table S1). In view of the lack of overlap in additional *Tnt1* flanking sequences recovered from the two lines (data not shown), these genes represent probable targets for control via *NST1*. This is further supported by the observation that the same set of genes with increased or reduced expression in both the *nst1-1* and *nst1-2* lines was also regulated similarly in the independent *nst1* point-mutation line.

Of the common downregulated genes in stems, 12 were involved in lignin biosynthesis, 17 were putatively involved in cellulose or hemicellulose biosynthesis, and 14 were tentatively involved in other aspects of cell wall formation, or with the cytoskeleton (Table 3). Quantitative real-time

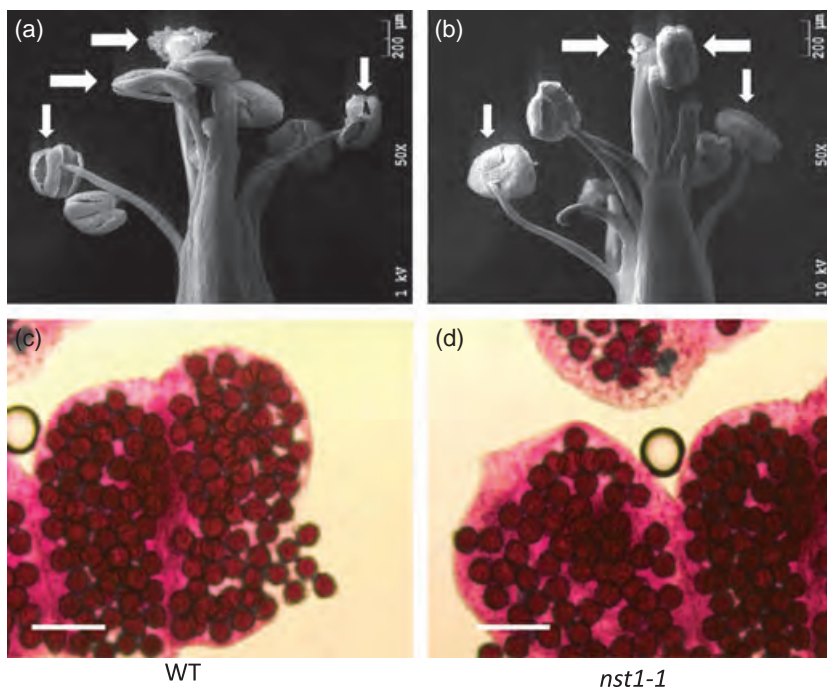


Figure 5. Mutation of *MtNST1* prevents anther dehiscence.

(a, b) Scanning electron micrographs showing anthers of wild-type (a) and *nst1-1* (b) flowers (7 days old). Wild-type anthers dehisced easily, and the stigma tops are covered by pollen. *nst* mutant anthers are closed in this late flowering stage and the stigma is empty of pollen.

(c, d) Pollen from wild-type (c) and *nst1-1* (d) stained with Alexander solution.

Scale bars: 200 μm in (a) and (b); 5 μm in (c) and (d).

PCR was used to validate microarray results. This indicated that the pattern of *MtNST1* expression paralleled that of lignin biosynthetic genes during stem development (Table 4), and that the expression of multiple genes involved in the biosynthesis of lignin, namely *FERULATE 5-HYDROXYLASE (F5H)*, *4-COUMARATE CoA LIGASE (4CL)*, *COUMAROYL SHIKIMATE 3-HYDROXYLASE (C3H)*, *HYDROXYCINNAMOYL CoA: SHIKIMATE HYDROXYCINNAMOYL TRANSFERASE (HCT)*, *CINNAMOYL CoA REDUCTASE (CCR)*, *CAFFEIC ACID 3-O-METHYLTRANSFERASE (COMT)* and *CAFFE OYL CoA 3-O-METHYLTRANSFERASE (CCoAOMT)* was indeed reduced in stems of the *nst1-1* mutant (Figure 6a). Genes with high sequence similarity to *IRREGULAR XYLEM 1 (IRX1)* and *FRAGILE FIBER 8 (FRA8)* were selected to represent genes potentially involved in the cellulose and hemicellulose synthesis pathways, respectively. As the identities of these two genes in *M. truncatula* have not yet been experimentally confirmed, three different primer pairs were chosen from each gene for quantitative real-time PCR (qRT-PCR) to ensure the accurate determination of gene expression: this confirmed that the expression levels of the *IRX1* and *FRA8* homologs were decreased in the *nst1* mutants (Figure 6b,c). The decreased expression of genes involved in secondary cell wall formation can explain the reduction of lignin and cell wall sugar in the *nst1* mutant, similar to the situation in the *Arabidopsis nst1:nst3* double mutant (Mitsuda *et al.*, 2007).

In addition to the inactivated *NST1* gene, probe sets annotated as encoding other transcription factors were also downregulated by more than twofold in *Mtnst1-1* and *Mtnst1-2* mutant lines, compared with controls: these

included two basic helix loop helix (*BHLH*) genes, two *NAC* genes and two *zinc finger protein* genes (Table S1). The two *NAC* genes are homologs of *Arabidopsis SND2*, and are in a different phylogenetic subgroup from *MtNST1* (Shen *et al.*, 2009). Neither of these genes contained a transposon insertion in any of the four independent *nst1* mutant alleles.

Because of the stomatal phenotype in leaf cells of the *nst1* mutants, we also performed microarray analysis with RNA samples from leaf panels (major veins removed) of wild-type and mutant plants. The loss of *MtNST1* function also has a major impact on polysaccharide biosynthesis gene expression in leaves (Table 3). The most downregulated genes were represented by eight cellulose synthase probe sets, in addition to arabinogalactan protein, peroxidase, glycoside hydrolase, chitinase-like and proline-rich protein. Five of the cellulose synthase probe sets were also downregulated in stems of the *nst1* mutant, three were only downregulated in leaves and two were only downregulated in stems. The arabinogalactan protein probe sets were downregulated in leaves but not stems of the *nst1* mutant. The other cell wall biosynthesis genes that were downregulated in stems of the *nst1* mutants were not downregulated in leaves (Table 3).

Saccharification potential of *Nst1* mutants

To evaluate the impact of cell wall changes on recalcitrance of biomass to saccharification, mature stems of *Mtnst1-1* and *Mtnst1-2* plants were subjected to dilute sulfuric acid pre-treatment and enzymatic hydrolysis with cellulases. Compared with the wild type, cell walls from the *nst1*

Table 3 Cell wall-related genes downregulated by more than twofold in stems and leaves of two independent *Medicago truncatula* *nst1* mutants

Probe set	Annotation	Transcript level relative to control			
		Stem		Leaf	
		<i>nst1-1</i>	<i>nst1-2</i>	<i>nst1-1</i>	<i>nst1-2</i>
Lignin biosynthesis					
Mtr.42553.1.S1_s_at	CYP84A1, FAH1 FAH1 (FERULATE-5-HYDROXYLASE 1); F5H	0.02	0.04	–	–
Mtr.20710.1.S1_at	Cytochrome P450 CYP84A1, FAH1 FAH1 (FERULATE-5-HYDROXYLASE 1)	0.03	0.05	–	–
Msa.1740.1.S1_at	FAH1 (FERULATE-5-HYDROXYLASE 1)	0.08	0.35	–	–
Mtr.10628.1.S1_at	CYP84A1, FAH1 FAH1 (FERULATE-5-HYDROXYLASE 1)	0.09	0.31	–	–
Mtr.39737.1.S1_at	LAC17 LAC17 (laccase 17); copper ion binding	0.18	0.02	–	–
Mtr.13653.1.S1_at	LAC17 (laccase 17); copper ion binding	0.19	0.04	–	–
Mtr.51876.1.S1_at	Peroxidase 64 (PER64) (P64) (PRXR4) e^{-138}	0.28	0.27	–	–
Mtr.4733.1.S1_s_at	Peroxidase 64 (PER64) (P64) (PRXR4) $4e^{-27}$	0.28	0.20	–	–
Mtr.4733.1.S1_at	Peroxidase 64 (PER64) (P64) (PRXR4) $4e^{-27}$	0.29	0.19	–	–
Mtr.42734.1.S1_at	LAC12 LAC12 (laccase 12); copper ion binding	0.47	0.19	–	–
Mtr.4126.1.S1_at	LAC17 LAC17 (laccase 17); copper ion binding	0.48	0.28	–	–
Mtr.43288.1.S1_at	IRX12, LAC4 IRX12/LAC4 (laccase 4); copper ion binding	0.28	0.23	–	–
Mtr.14592.1.S1_at	Peroxidase	–	–	0.22	0.24
Mtr.40132.1.S1_at	Peroxidase	–	–	0.47	0.42
Cellulose biosynthesis					
Mtr.33788.1.S1_at	IRX7, FRA8 FRA8 (FRAGILE FIBER 8)	0.28	0.41	–	–
Mtr.50224.1.S1_s_at	IRX3 (IRREGULAR XYLEM 3) cellulose synthase	0.36	0.30	0.41	0.46
Mtr.40320.1.S1_at	IRX7, FRA8 FRA8 (FRAGILE FIBER 8)	0.38	0.42	–	–
Mtr.33547.1.S1_at	CESA8, IRX1, ATCESA8, LEW2 CESA8 (CELLULOSE SYNTHASE)	0.42	0.34	–	–
Mtr.5242.1.S1_at	CESA8, IRX1, ATCESA8, LEW2 CESA8 (CELLULOSE SYNTHASE 8); $4e^{-65}$	0.42	0.37	0.32	0.35
Mtr.13202.1.S1_at	CESA8, IRX1, ATCESA8, LEW2 CESA8 (CELLULOSE SYNTHASE 8)	0.43	0.36	0.29	0.32
Mtr.10615.1.S1_at	ATCESA7, CELLULOSE SYNTHASE CATALYTIC SUBUNIT 7, CESA7, IRREGULAR XYLEM 3	0.47	0.39	0.44	0.46
Mtr.11798.1.S1_at	CESA8, IRX1, ATCESA8, LEW2 CESA8 (CELLULOSE SYNTHASE 8)	0.48	0.41	0.37	0.37
Mtr.37806.1.S1_at	CESA4, IRX5, NWS2 CESA4 (CELLULOSE SYNTHASE A4)	–	–	0.31	0.35
Mtr.5274.1.S1_s_at	CESA4, IRX5, NWS2 CESA4 (CELLULOSE SYNTHASE A4)	–	–	0.20	0.19
Mtr.51462.1.S1_s_at	CESA4, IRX5, NWS2 CESA4 (CELLULOSE SYNTHASE A4)	–	–	0.24	0.24
Hemicellulose/pectin biosynthesis					
Mtr.39454.1.S1_at	ATFXG1 ATFXG1 (ALPHA-FUCOSIDASE 1) able to release the <i>t</i> -fucosyl residue from the side chain of xyloglucan	0.03	0.09	–	–
Mtr.25494.1.S1_at	ATGOLS1 ATGOLS1 (ARABIDOPSIS THALIANA GALACTINOL SYNTHASE 1); transferase, transferring hexosyl groups	0.07	0.39	–	–
Mtr.41429.1.S1_at	GATL1, PARVUS, GLZ1 GATL1/GLZ1/PARVUS GALACTURONOSYL TRANSFERASE-LIKE 1); polygalacturonate 4-alpha-galacturonosyltransferase/transferase e^{-169}	0.35	0.35	–	–
Mtr.41311.1.S1_at	GAUT12, LGT6, IRX8 GAUT12/IRX8/LGT6 GALACTURONOSYLTRANSFERASE 12; polygalacturonate 4-alpha-galacturonosyltransferase $3e^{-163}$	0.38	0.31	–	–
Mtr.30695.1.S1_at	GAUT12, LGT6, IRX8 GAUT12/IRX8/LGT6 GALACTURONOSYLTRANSFERASE 12; polygalacturonate 4-alpha-galacturonosyltransferase	0.39	0.31	–	–
Mtr.24892.1.S1_at	ATBXL2, BXL2 BXL2 (BETA-XYLOSIDASE 2); hydrolase involved in secondary wall hemicellulose metabolism	0.43	0.28	–	–
Mtr.32451.1.S1_s_at	ATBXL2, BXL2 BXL2 (BETA-XYLOSIDASE 2); hydrolase	0.45	0.28	–	–
Mtr.38262.1.S1_at	IRX14 IRX14 (IRREGULAR XYLEM 14); glycosyl transferase that contributes to xylan biosynthesis	0.46	0.37	–	–
Mtr.5557.1.S1_at	Glycosyl hydrolase family 3 protein $1e^{-68}$ same family as bxl2 and bxl3	0.49	0.47	–	–
Other cell wall related					
Mtr.10992.1.S1_at	Arabinogalactan protein like	–	–	0.11	0.10
Mtr.15775.1.S1_at	Glycoside hydrolase	–	–	0.39	0.36
Mtr.24717.1.S1_s_at	Arabinogalactan protein-like	–	–	0.32	0.33
Cytoskeleton					
Mtr.35578.1.S1_at	ATMAP70-2, F5A9.19, F5A9_19, MICROTUBULE-ASSOCIATED PROTEIN 70-2	0.39	0.35	–	–
Mtr.44524.1.S1-at	ARPC2B ARPC2B (actin-related protein C2B), structural molecule; similar to ARPC2A/DIS2 (DISTORTED TRICHOMES 2)	0.41	0.35	–	–
Mtr.39566.1.S1_at	Kinesin light chain-related	0.43	0.41	–	–
Mtr.39117.1.S1_at	Kinesin light chain-related	0.43	0.39	–	–
Mtr.18524.1.S1-at	KATC, ATK3 ATK3 (ARABIDOPSIS THALIANA KINESIN 3); microtubule motor	0.46	0.36	–	–

Probe set	Annotation	Relative transcript level		
		Internode 2	Internode 3	Internode 5
Mtr.33913.1.S1_at	NST1	41 ± 0.9	131 ± 28	477 ± 68
Mtr.40238.1.S1_at	HCT	3315 ± 187	5108 ± 971	15 782 ± 1155
Mtr.13904.1.S1_at	4CL	19 ± 2	33 ± 7	580 ± 101
Mtr.8589.1.S1_at	CAD	1437 ± 317	2601 ± 498	8704 ± 302
Mtr.43183.1.S1_at	C3H	3603 ± 355	5274 ± 579	8792 ± 285

Transcript level is expressed relative to actin.

mutants released more glucose and less xylose during sulfuric acid pre-treatment (Figures 7a and S12). Without pre-treatment, the cellulase mixture could release 64% of the structural sugars from the *nst1-1* mutant, significantly higher than in the wild type (46%). Following acid pre-treatment, enzymatic hydrolysis could release 90% of the total sugars (723 mg sugar per gram of cell wall residue) from *nst1-1* compared with 67% (572 mg sugar per gram cell wall residue) from the wild type (Figure 7b). Similar results were obtained with a second allele (*nst1-2*) (Figure S12).

DISCUSSION

Loss of function of a single NAC gene impacts lignification in *Medicago*

We have identified an NAC family transcription factor, MtNST1, from UV microscopy-based screening for secondary cell wall formation defects in an *M. truncatula* mutant collection generated by tobacco *Tnt1* retrotransposon insertion mutagenesis. Four independent *nst1* mutants all show secondary cell wall formation defects in stems, anther dehiscence defects, and reduced ferulic acid fluorescence in stomatal guard cell walls. The *nst1* mutants phenocopy the recently reported Arabidopsis *nst1:nst3* double mutant and *nst1:nst2* double mutant, as regards the stem and anther phenotypes, respectively (Mitsuda *et al.*, 2007; Zhong *et al.*, 2007), but the guard cell phenotype has not been reported previously.

Unlike Arabidopsis, which contains three partially redundant *NST* genes, *M. truncatula* only appears to possess one *NST* gene. *M. truncatula* NST1 shares high sequence similarity with its Arabidopsis counterparts, but only in the conserved N-terminal NAC domain. A recently published phylogenetic analysis of 1232 NAC proteins from 11 different plants places the proteins into eight subfamilies, which are then divided into different clades based on motif patterns in the highly diverse C-terminal regions (Shen *et al.*, 2009). MtNST1 and the three Arabidopsis *NST* proteins all fall into the NAC-c subfamily, subgroup c-3. Interestingly, *Medicago* is the only organism with a single representative NAC protein in the C-3 subfamily.

The *M. truncatula nst1* mutants have severe secondary wall biosynthesis defects, whereas none of the single

Table 4 Quantitative real-time PCR analysis of *NST1* and lignin pathway gene transcripts in *Medicago truncatula* stem internodes at different developmental stages (from 50-day-old plants)

Arabidopsis *NST* gene knock-outs shows such phenotypes. Redundancy appears to be a common theme for other genes involved in cell wall component biosynthesis. For example, 10 *CesA* (cellulose synthase) genes are present in Arabidopsis, and poplar has 18 (Djerbi *et al.*, 2005; Keegstra and Walton, 2006). At least nine cinnamyl alcohol dehydrogenase (CAD) enzymes catalyzing reduction of various phenylpropenyl aldehyde derivatives in lignin biosynthesis have been functionally characterized in Arabidopsis (Kim *et al.*, 2004). Arabidopsis *CAD4* and *CAD5* are functionally redundant, and only a double knock-out shows striking lignin reduction (Sibout *et al.*, 2005). A *cad1* mutant from *M. truncatula* shows severe lignin reduction when the single gene is disrupted, indicating that, like *MtNST1*, *CAD1* also does not have a second functionally redundant gene family member in *Medicago* (Q. Zhao, F. Chen and R.A. Dixon, unpublished data). Overall, however, phenylpropanoid pathway gene families are as complex, or more complex, in *Medicago* than in Arabidopsis: for example, Arabidopsis possesses a single functional chalcone synthase (*CHS*) gene, whereas the *Medicago CHS* gene family contains at least 23 members.

MtNST1 orchestrates cell wall synthesis in multiple cell types

Based on the microarray analysis of gene expression patterns at different developmental stages of stems, *MtNST1* is expressed at a very low level in early stages, when most cells are still dividing and expanding. The expression level increases as cells mature, in parallel with the expression of lignin biosynthetic genes.

Knock-out of *MtNST1* appears to block the development of secondary cell walls in the interfascicular region of the stem, and in the phloem fibers, and may also lead to a reduction of total lignin in xylem vessel cell walls. However, the loss of fluorescence and ferulate-related CARS signal from the guard cell walls in all of the *nst1* mutants suggests that *NST1* may also control modification of primary cell walls in guard cells. Substitution of the arabinan portion of pectin with ferulic acid is essential for providing the necessary physical properties to guard cell walls, to allow for the expansion and contraction necessary for stomatal opening and closing (Jones *et al.*, 2003), and the removal of ferulates

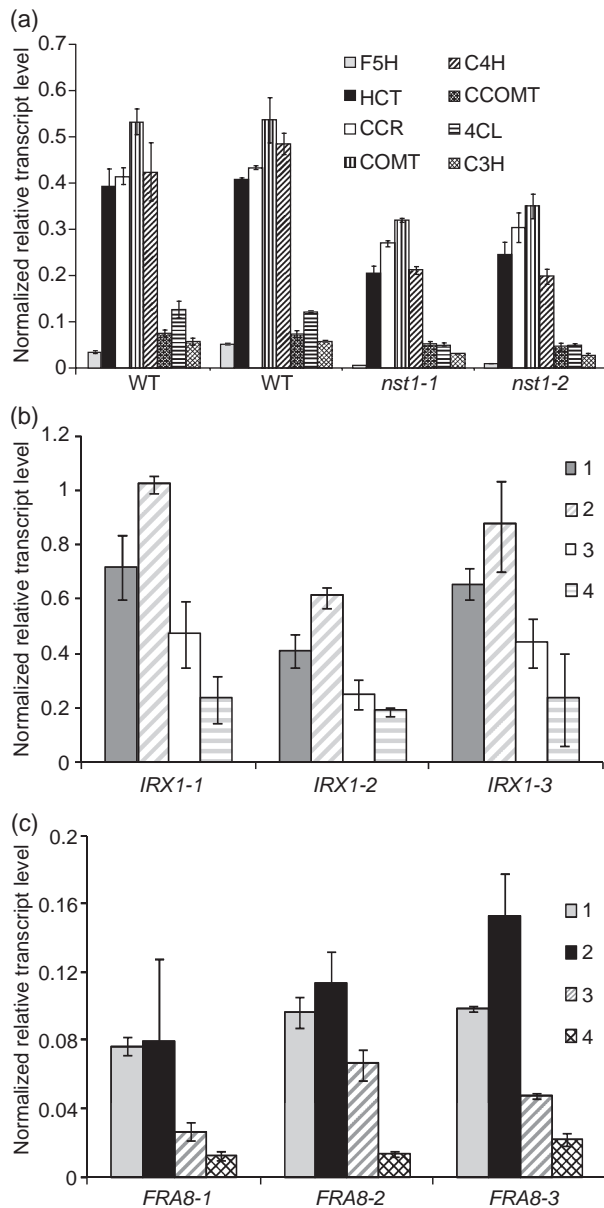


Figure 6. Levels of cell wall biosynthetic gene transcripts in the wild type and *nst1-1* and *nst1-2* mutants, as determined by quantitative real-time PCR (qRT-PCR).

(a) Expression of genes related to lignin biosynthesis. Data are means and SDs of triplicate assays.

(b, c) Expression of putative *IRX1* (b) and *FRA8* (c) genes. Transcript levels were measured with three different primer pairs. Data are means and SDs of triplicate assays.

In (b) and (c), 3 and 4 are data for *nst1-1* and *nst1-2*, respectively, and 1 and 2 are the corresponding control lines.

from guard cell walls by incubation of epidermal strips with feruloyl esterase results in an inability of guard cells to open properly (Jones *et al.*, 2005). This is exactly mirrored by the phenotype of the *nst1* mutants, in which guard cell aperture is dramatically reduced.

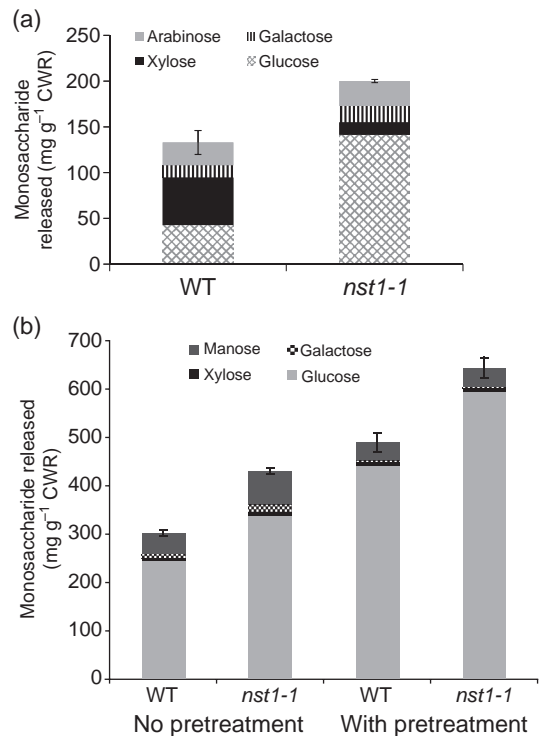


Figure 7. Sugar release from cell walls of wild-type *Medicago truncatula* and the *nst1-1* mutant by chemical and enzymatic saccharification.

(a) Saccharification efficiencies after dilute acid pre-treatment.

(b) Enzymatic saccharification efficiencies with and without acid pre-treatment.

The CARS analysis provides spatial and semi-quantitative information on ferulate levels in the stomatal complex. Direct measurement of pectin-linked ferulate levels in guard cells of *nst1* mutants, compared with wild-type *M. truncatula* will probably require laser capture microdissection, a technique that we have recently used for analysis of cell type-specific deposition of lignin in transgenic alfalfa (Nakashima *et al.*, 2008).

The lack of significant reduction in the total leaf wall-bound ferulate pool in the *nst1* mutants, despite the total loss of guard cell wall fluorescence, can be readily explained by the low frequency of guard cells in the samples. This would also explain our inability to detect changes in pectin-related cell wall biosynthetic gene transcripts in microarray analysis of transcripts from whole leaf panels. It is possible that the loss of function of *MtNST1* also leads to a loss of wall-bound ferulate in the interfascicular region of the stem: this would not be observed because of the massive autofluorescence from lignin in wild-type plants.

We cannot rule out the possibility that the reduction in the stomatal aperture response in *nst1* mutants might also result from disruptions to other cell wall components, such as cellulose, as suggested by the downregulation of a

specific class of putative cellulose synthase genes in *nst1* mutant leaves.

Potential downstream targets for *NST1* action

In addition to the downregulation of over fifty genes involved in the biosynthesis of the major components of the secondary cell wall, genes encoding six putative transcription factors were either down- or upregulated in stems of two independent *Mtnst-1* mutant lines. Previous work from Arabidopsis has suggested that *NST* genes function as master switches of a transcriptional network involved in the regulation of secondary wall biosynthesis, and several transcription factors have been shown to be regulated by *NST* genes (Zhong *et al.*, 2008; Zhou *et al.*, 2009). Among the six transcription factors with modified expression in the *nst1* mutants, one is the homolog of *AtMYB103*, which was previously reported to be regulated by *AtNST1* and *NST3* (Zhou *et al.*, 2009). The other transcription factors include two *NAC* genes, two Dof-type zinc finger domain-containing genes and one homeobox gene. These could potentially control downstream branches of the secondary wall biosynthesis pathway in Medicago. For example, the two *NAC* genes downregulated as a result of loss of *MtNST1* function are homologs of *AtSND2*, which is a downstream target of *NST1* in Arabidopsis (Zhong *et al.*, 2008). The zinc finger and homeodomain genes represent novel candidates for cell wall regulation.

The transcript levels of two putative laccases were decreased as a result of the *NST1* downregulation in stems. An additional microarray analysis using RNA samples from different developmental stages indicates that the two laccases exhibit a similar expression pattern to that of lignin biosynthetic genes (H. Wang, Q. Zhao, F. Chen and R.A. Dixon, unpublished data). Despite many years of effort, no specific laccase genes have been unequivocally demonstrated to be involved in lignin polymerization. The finding that the two laccases are regulated by *MtNST1*, and that they have similar developmental expression patterns as lignin genes, suggests that both laccases are potentially involved in lignin polymerization.

MtNST1 as a target for development of alfalfa as a bioenergy crop

Mutation of *MtNST1* in *M. truncatula* resulted in the abolition of lignification in interfascicular and phloem fibers, and is likely to affect other aspects of secondary cell wall synthesis in these fiber cells. Cell wall xylose levels were significantly reduced, which probably reflects changes in the hemicellulose component of the secondary cell wall. The overall consequence of these changes in cell wall composition is that the mutant is more amenable to chemical and enzymatic treatment for release of sugars for ethanol fermentation. Whereas the lower level of xylose in the pre-treatment hydrolysate is likely to result from impaired

biosynthesis of hemicelluloses in *nst1* mutants, the increased glucose content may be caused by the decreased crystallinity of cellulose.

Knock-out of *NST1* in *M. truncatula* greatly improved the enzymatic hydrolysis efficiency of cell walls with or without acid pre-treatment. Similar to our previous report on transgenic plants modified in the monolignol biosynthetic pathway (Chen and Dixon, 2007), the sugar release efficiency of cell walls from mutants that were not pre-treated is close to that of the pre-treated wild type cell walls. Recent studies indicate that biomass from *NST*-downregulated Arabidopsis plants is approximately twice as efficiently processed by enzymatic and physicochemical treatments as is biomass from control plants (Iwase *et al.*, 2009). The fact that the walls from the mutants are more responsive to chemical and enzymatic treatment suggests that milder pre-treatment or lower enzyme loading could be used to release sugar from these materials. Although there is a small overall reduction in cell wall polysaccharide in the *Mtnst1* mutants, this is more than compensated for as regards saccharification yields by the reduction in lignin content. Furthermore, the growth reductions observed in lines harboring a complete knock-out of *NST1* are significantly less than those observed in transgenic plants, in which saccharification efficiency is similarly improved through the knock-down of monolignol biosynthetic enzymes (Chen and Dixon, 2007).

Our results clearly demonstrate the potential of *NST1* as a target for genetic engineering of plant cell walls for bioenergy feedstock improvement. Furthermore, *NST1* downregulation has the added advantage (from the transgenic release perspective) of resulting in pollen containment, and the consequent lack of seed production in the self-pollinating *M. truncatula* resulting from the impairment of anther dehiscence; it is, however, easy to obtain pollen for crossing during breeding through manual dehiscence of the anthers. Full exploitation of *nst1* mutants for bioenergy and/or forage crop development might, however, require crossing into lodging tolerant genetic backgrounds to compensate for the weakened stems as a result of the blocked development of the fiber cell walls.

EXPERIMENTAL PROCEDURES

Plant materials and growth conditions

A tobacco (*Nicotiana tabacum*) *Tnt1* retrotransposon-tagged mutant collection of *M. truncatula* (Tadege *et al.*, 2005, 2008) was screened for defects in secondary cell wall formation. Plants were grown in MetroMix 350 soil mix at 24°C during the day and 20°C during the night, with a 16-h day/8-h night photoperiod, 70–80% relative humidity, and 150 $\mu\text{mol m}^{-2} \text{sec}^{-1}$ light intensity. Sixth internodes of each plant were harvested when the plants had reached around eight internodes, and were stored at –80°C.

Four *nst1* alleles were identified from forward and reverse genetic screening of a segregating population of just over 9000 independent R1 lines.

Identification and molecular cloning of *MtNST1*

To identify the gene that is linked to the lack-of-lignification phenotype, total RNA samples from fifth to eighth internodes were subjected to Affymetrix microarray analysis, as described below. Segregating progeny without the loss-of-lignification phenotype from the same parent plant as the mutants were used as control. Downregulated probe sets were chosen as candidates for RT-PCR analysis, prioritized in order of the extent of downregulation, as compared with lines segregating with the wild-type phenotype. PCR was performed using *Tnt1* (forward primer, 5'-TCCTTGTTG GATTGGTAGCCAACCTTTGTTG-3'; reverse primer, 5'-AGTTGGCTA CCAATCCAACAAGGA-3') and gene specific primers to confirm that the insertion was linked to the phenotype.

To clone the full-length *NST1* gene, BLAST analysis of the *M. truncatula* genome from DFCI (<http://compbio.dfci.harvard.edu/cgi-bin/tgi/gimain.pl?gudb=medicago>) was performed using Mtr.33913.1.S1_at as the query probe sequence: this led to a partial cDNA sequence. The sequence was completed by 3' RACE using the SMART RACE cDNA Amplification Kit (Clontech, <http://www.clontech.com>) using the *NST1* forward primer (5'-CCCTAGACAGCC CTTCTGGAGAGGGGAAGAAGCC-3') to complete the 3' end of the *NST1* cDNA. The *NST1* genomic sequence was also PCR amplified and sequenced from *M. truncatula* ecotype R108.

To confirm *NST1* as the disrupted gene causing the lignification phenotype, reverse genetic screening was performed to uncover additional alleles. Genomic DNA was extracted from individual lines and pooled together with 500 independent lines, contributing to one super pool. PCR screening of superpools, and subsequently the screening of smaller pools to individual lines, was performed using the *Tnt1* forward primer 5'-TCCTTGTTGGATTGGTAGCCAACCTT-GTTG-3', the *Tnt1* reverse primer 5'-AGTTGGCTACCAATCCAACA-AGGA-3' and two pairs of *NST1* gene-specific primers.

Sequence comparisons

MEGALIGN protein alignment software (DNASTAR, <http://www.dnastar.com>) was used for multiple sequence alignments using the CLUSTAL algorithm.

Identification of *Tnt1* insertion sites in *MtNST1*

The *Tnt1* flanking sequences from the *nst1-1*, *nst1-2*, *nst1-3* and *nst1-4* alleles were PCR amplified using a combination of the *NST1* forward primer (5'-ATGCCTGATAACATGAGTATATCTGTTAATG-GAC-3') and the *Tnt1* primer above. The PCR product sequences were aligned with the *NST1* genomic DNA sequence to determine the retrotransposon insertion sites.

Phenotypical analysis and physiological measurements

All measurements were performed on plants of *M. truncatula* at the time when the first flower appeared. Six stems were harvested for each line. The number and lengths of internodes and total stem length were recorded, and their means analyzed in EXCEL (Microsoft, <http://www.microsoft.com>). Leaf area was measured using a LI-3000A portable area meter (LI-COR, <http://www.licor.com>), and stem diameter was measured using an automatic calibrator (Fisher Scientific, <http://www.fishersci.com>).

Photosynthesis and transpiration rates were determined using an LI-6400 infra-red CO₂ gas analyzer (LI-COR). Cylinders of pre-mixed gases were supplied by LI-COR. Measurements were made at a light intensity of 600 $\mu\text{mol m}^{-2} \text{sec}^{-1}$, a leaf temperature of 22°C and a vapor pressure deficit of 0.7 kPa. A fluorescence chamber head (LI-6400-40; LI-COR) was integrated with the LI-6400 open gas exchange system to measure steady-state fluorescence (F_s) and

maximum fluorescence during a light-saturating pulse (F_m). The photochemical quantum yield of electron transport through photosystem II (PSII) was calculated as $\Phi_{\text{PSII}} = (F_m - F_s)/F_m$ (Genty *et al.*, 1989). All measurements were performed on two different days from 11:00 until 13:00 h in the glasshouse chamber.

Scanning electron microscopy

Samples were vacuum infiltrated with 3% glutaraldehyde in 1xPBS overnight at 4°C, then washed four times with fresh PBS solution. Post-fixation was in 1% osmium tetroxide in H₂O for 2 h on ice, followed by washing in fresh PBS solution. Samples were dehydrated in an ethanol series from 50 to 100%, then placed in 100% tert-butanol and freeze dried. Dried samples were mounted on aluminum stubs, and petals of individual flowers were removed manually. The samples were then sputter-coated with gold palladium. Flower structures were examined under a Zeiss DSM-960A SEM at an accelerating voltage of 5 kV. Digital photographs were collected and assembled using PHOTOSHOP (Adobe, <http://www.adobe.com>).

Analysis of stomata

Epidermal cells strips were peeled with nail varnish from mature leaves of 8-week-old plants. The thin film was peeled off from the leaf surface, mounted on a glass slide and observed under the microscope. For measurement of stomatal opening, the plants were kept at 20°C in the dark for 1 h, and then transferred to light for 2 h. Epidermal cell film strips were taken under both conditions, and observed directly under the microscope. Strips harvested during the dark phase were kept in 10 mM KCl, and those harvested in the light were kept in 75 mM KCl. Stomatal aperture was defined as the ratio between the length and the width of guard cells (in μm). A ratio of 1 indicates the maximum opening potential of the stomatal pore. Length analysis was performed using IMAGEJ (<http://rsbweb.nih.gov/ij>).

For CARS microscopy, we used a mode-locked Nd:VAN laser (High Q Laser, Inc., <http://www.highqlaser.at>) to generate 7-ps, 76-MHz pulse trains of both 1064- and 532-nm laser beams. The 1064-nm beam was used directly as the Stokes beam. The 532-nm beam pumped an optical parametric oscillator (OPO) (Levante Emerald; APE-Berlin, <http://www.ape-berlin.de>) to generate the CARS pump beam. The pump beam was tuned to 910 nm to effectively detect the 1600-cm⁻¹ Raman band. Collinear and temporally overlapped pump and Stokes beams were focused onto the sample by an Olympus UPlanSapo 60x water immersion objective (<http://www.olympus-global.com>). Epidermal layers of the leaves were carefully peeled off and spread out between two coverslips. The CARS images of ferulate in this epidermal layer were obtained at 1600 cm⁻¹ on an Olympus IX 81 microscope. The focused beams were raster scanned over the sample. The anti-Stokes light was collected from the Epi-direction and filtered by a clean-up filter 800/40 (Thorlabs, <http://www.thorlabs.de>). Each time, an off-resonance image at 1550 cm⁻¹ was also acquired and subtracted from the 1600 cm⁻¹ image to remove the non-resonance background.

Fluorescence microscopy

The second to fifth internodes, counting from the top of stems, of wild-type *M. truncatula* and *nst1* mutants were cross-sectioned to 100 μm using a Leica RM 2255 Microtome (<http://www.leica.com>). For UV-fluorescence microscopy, the UV intensity was kept constant between samples. Sections were observed under the Nikon Microphot-FX system with a Nikon DXM 1200 color camera (<http://www.nikon.com>).

Pollen staining

To determine pollen viability, flowers were picked at similar stages from wild-type and *nst1* mutant *M. truncatula*. Entire flowers were incubated in Carnoy's fixative for 1 h at room temperature, and then transferred to Alexander solution (Alexander, 1969) for 4 h at room temperature. The flowers were then de-stained in 10% glycerol for 30 min prior to observation.

Microarray analysis

Total RNA was isolated with Tri-reagent according to the manufacturer's protocol (Invitrogen, <http://www.invitrogen.com>). RNA was prepared from stem or leaf tissue from 2-month-old plants. Veins were removed from leaf tissue prior to RNA isolation. RNA was cleaned and concentrated using the RNeasy MinElute Cleanup Kit (Qiagen, <http://www.qiagen.com>) and 10 µg of purified RNA was used for microarray analysis of three biological replicates. In both stem and leaf microarrays, RNA was isolated from two independent mutant alleles (*nst1-1* and *nst1-2*). Probe labeling, hybridization and scanning for microarray analysis were conducted according to the manufacturer's instructions (Affymetrix, <http://www.affymetrix.com>). Data normalization was conducted using robust multi-chip average (RMA) (Irizarry *et al.*, 2003). The presence/absence call for each probe set was obtained from dCHIP (Li and Wong, 2001). Genes with significantly different expression levels between the wild-type control and mutants were selected using associative analysis, as described by Dozmorov and Centola (Dozmorov and Centola, 2003). The type-I family-wise error rate was reduced by using a Bonferroni corrected *P*-value threshold of 0.05/*N*, where *N* represents the number of genes present on the chip. The false discovery rate was monitored and controlled by *Q* value (false discovery rate), calculated using Extraction of Differential Gene Expression (EDGE, <http://www.biostat.washington.edu/software/jstorey/edge>) (Storey and Tibshirani, 2003; Leek *et al.*, 2006).

Real-time PCR

cDNA samples were used for qRT-PCR, with technical duplicates. The 10-µl reaction included 2 µl of primers (0.5 µM of each primer), 5 µl Power Sybr (Applied Biosystems, <http://www.appliedbiosystems.com>), 2 µl of 1:20 diluted cDNA from the reverse transcription step and 1 µl of water. qRT-PCR data were analyzed using SDS 2.2.1 (Applied Biosystems). The PCR efficiency was estimated using LINREGPCR (Ramakers *et al.*, 2003), and the transcript levels were determined by relative quantification (Pfaffl, 2001) using the *M. truncatula* actin gene as a reference.

Determination of lignin content and composition

The lignin content of stem material (internodes 5–8) was determined by the acetyl bromide method using ~15 mg of extractive-free material (Hatfield *et al.*, 1999). The same molar extinction coefficient of 17.2 (as determined for lignin from wild-type alfalfa) was used for samples of all the transgenic lines.

Lignin composition was determined by thioacidolysis (Lapierre *et al.*, 1985, 1995). Approximately 15–20 mg of extractive-free samples was reacted with 15 ml of 0.2 M BF₃ etherate in an 8.75:1 dioxane/ethanethiol mixture. Lignin-derived monomers were identified by gas chromatography mass spectrometry (GC/MS), and quantified by GC as their trimethylsilyl derivatives. GC/MS was performed on a Hewlett-Packard 5890 series-II gas chromatograph with a 5971 series mass selective detector (column:HP-1; 60 m × 0.25 mm; 0.25-µm film thickness; <http://www.hp.com>), and mass spectra were recorded in electron impact mode (70 eV) with a 60–650 *m/z* scanning range.

Profiling of soluble and wall-bound phenolics

Glasshouse-grown stem samples were collected from two independent mutant alleles (*nst1-1* and *nst1-2*). The top second to ninth stem internodes were harvested from three individual mutants and corresponding heterozygous control plants, and ground under liquid nitrogen. For soluble phenolics, freeze-dried samples (100 mg) were incubated with 2 ml of chloroform/methanol (2:1, v/v) at room temperature overnight with gentle shaking. The samples were incubated on the shaker for another 4 h at room temperature. After centrifugation at 12 000 *g* for 10 min, the supernatant (methanol/water fraction) was taken for HPLC profiling of soluble phenolics.

For analysis of wall-bound phenolics, the cell wall residues were further extracted with 100% methanol, 50% methanol and water (three times each), and then freeze dried. Freeze-dried cell wall residue (60 mg) was hydrolyzed with aqueous 2 N NaOH (1.8 ml) at 37°C for 5 h in the dark. The mixtures were acidified to pH 3 with 1:1 (v/v) HCL (600 µl). After extraction with ethyl acetate (1.6 ml × 3), the combined organic phases were dried under a stream of N₂ and re-suspended in 300 µl 70% methanol for HPLC analysis.

Compounds were identified by comparing the UV spectra and retention times with those of authentic standards, and quantified by means of standard curves. HPLC was carried out on a Beckman System Gold HPLC system, consisting of a programmable solvent module 126, a System Gold 508 autosampler and a System Gold 168 diode array detector (<http://beckman-coulter.com>). A Phenomenex Luna 5µ C18 reverse phase column (5-µm particle, 250 × 4.6 mm) was used (<http://www.phenomenex.com>): solvent A, 0.1% phosphoric acid in water; solvent B, acetonitrile. The gradient for soluble phenolics was: 8% B for 1 min; 8% B to 35% B in 45 min; at 46 min, B from 35% to 100% in 1 min. The gradient for wall-bound phenolics was: 8% B for 1 min; 10% B to 27% B in 50 min; at 51 min, B from 27% to 100% in 1 min.

Analysis of cell wall sugar levels and composition

The determination of carbohydrates was conducted according to the Laboratory Analytical Procedure of the National Renewable Energy Laboratory (LAP-019). Biomass (~300 mg) was first hydrolyzed in 72% sulfuric acid at 30°C, then in dilute acid (4%) at 130°C for 1 h. The solubilized sugars were analyzed spectrophotometrically using the phenol-sulfuric acid assay (Dubois *et al.*, 1956). Mono-saccharide compositions were determined by HPLC (Agilent 1200 Series LC System with 1200 Series Refractive Index Detector; Agilent, <http://www.chem.agilent.com>). An Aminex HPX-87P column was used at 70°C, and the sugars were eluted with Milli-Q filtered water at a flow rate of 0.6 ml min⁻¹. The detector temperature was 50°C. Peaks were identified and quantified by comparison with authentic standards.

Chemical pre-treatment and enzymatic saccharification

Dried stem material at a solid loading of 2% (w/w) was mixed with dilute sulfuric acid (final concentration 1.5%, w/w) and pre-treated in an autoclave at 130°C for 2 h. After pre-treatment, the hydrolysates were separated and collected by filtration from residual biomass, and the biomass residues were washed with water. For enzymatic hydrolysis, Celluclast 1.5 L (cellulase from *Trichoderma reesei*) and Novozyme 188 (cellobiase from *Aspergillus niger*) (Sigma-Aldrich, <http://www.sigmaaldrich.com>) were mixed (equal volumes) and used at a loading of 31.5 filter paper units per g cell wall residue. Enzymatic saccharification of lignocellulosic material was performed according to the Laboratory Analytical Procedure of the National Renewable Energy Laboratory (LAP-009). About 0.125 mg of cell wall residues were hydrolyzed with a cellulase/cellobiase mix in a total volume of 10 ml by adding appropriate quantities of

enzyme mixture and sodium citrate buffer (0.1 M, pH 4.8) for 72 h. Enzyme blanks and Whatman #1 filter paper were digested alongside the samples (<http://www.whatman.com>). Hydrolysis of filter paper was always more than 95%. The total sugar and sugar composition in hydrolysates from chemical pre-treatment and enzymatic hydrolysis were determined using the phenol-sulfuric acid assay and HPLC, as described above.

ACKNOWLEDGEMENTS

We thank Lisa Jackson, Gail Shadle, and Liying Qi for assistance with mutant screening and lignin analyses, Drs Jiangqi Wen and Xiaofei Cheng for forward and reverse genetic screening, Dr Yuhong Tang for microarray analysis, and Drs Jin Nakashima, Elison Blancaflor and Li Quan for help with pollen staining and light microscopy, Dr Scott Russell (University of Oklahoma) for assistance with SEM analysis, and Drs Rujin Chen, Catalina Pislariu and Jianghua Chen for their critical reading of the manuscript. The *M. truncatula* plants utilized in this research project, which are jointly owned by the Centre National de la Recherche Scientifique, Gif-sur-Yvette, France, and the Samuel Roberts Noble Foundation, Ardmore, OK, USA, were created through research funded, in part, by grant 703285 from the National Science Foundation. This work was supported by grants to RAD from the USDA-DOE Feedstock Genomics program (award number DE-FG02-06ER64303) and the State Regents of Oklahoma (Oklahoma Bioenergy Center), the US Department of Energy Bioenergy Research Centers, through the Office of Biological and Environmental Research in the DOE Office of Science, and by the Samuel Roberts Noble Foundation.

SUPPORTING INFORMATION

Additional Supporting Information may be found in the online version of this article:

Figure S1. Cell wall phenotypes of *Tnt1* mutants.

Figure S2. Cross sections of the sixth internodes of wild-type and *nst1-1 Medicago truncatula*, showing the phloem tissues.

Figure S3. Protein sequence alignments of MtNST1 with Arabidopsis NST3.

Figure S4. Lignin deposition defects in additional independent *nst1* mutants.

Figure S5. Thioacidolysis yields of individual lignin monomers from stems of wild-type and *nst1* mutant *Medicago truncatula*.

Figure S6. Wall-bound phenolic content of wild-type and *nst1* mutant *Medicago truncatula*.

Figure S7. HPLC profiles of soluble phenolic compounds in wild-type and *nst1* mutant *Medicago truncatula*.

Figure S8. Stem phenotypes of wild-type and *nst1* mutant *Medicago truncatula*.

Figure S9. Stem growth of control and *Medicago nst1* mutant lines.

Figure S10. Guard cell phenotypes of homozygous and heterozygous *nst-1* mutant alleles.

Figure S11. High magnification SEM pictures of wild-type and *nst1* mutant flower parts.

Figure S12. Sugar release from cell walls of wild-type *Medicago truncatula* and the *nst1-2* mutant by chemical and enzymatic saccharification.

Table S1. Genes that are up- and downregulated by more than twofold in two independent *nst1* mutants, compared with the wild type.

Please note: As a service to our authors and readers, this journal provides supporting information supplied by the authors. Such materials are peer-reviewed and may be re-organized for online delivery, but are not copy-edited or typeset. Technical support

issues arising from supporting information (other than missing files) should be addressed to the authors.

REFERENCES

- Alexander, M.P. (1969) Differential staining of aborted and nonaborted pollen. *Stain Technol.* **44**, 117–122.
- Benedito, V.A., Torres-Jerez, I., Murray, J.D. *et al.* (2008) A gene expression atlas of the model legume *Medicago truncatula*. *Plant J.* **55**, 504–513.
- Boerjan, W., Ralph, J. and Baucher, M. (2003) Lignin biosynthesis. *Annu. Rev. Plant Biol.* **54**, 519–546.
- Carroll, A. and Somerville, C. (2009) Cellulosic biofuels. *Annu. Rev. Plant Biol.* **60**, 165–182.
- Chen, F. and Dixon, R.A. (2007) Lignin modification improves fermentable sugar yields for biofuel production. *Nat. Biotechnol.* **25**, 759–761.
- Chen, F., Reddy, M.S.S., Temple, S., Jackson, L., Shadle, G. and Dixon, R.A. (2006) Multi-site genetic modulation of monolignol biosynthesis suggests new routes for formation of syringyl lignin and wall-bound ferulic acid in alfalfa (*Medicago sativa* L.). *Plant J.* **48**, 113–124.
- Djerbi, S., Lindskog, M., Arvestad, L., Sterky, F. and Teeri, T.T. (2005) The genome sequence of black cottonwood (*Populus trichocarpa*) reveals 18 conserved cellulose synthase (CesA) genes. *Planta*, **221**, 739–746.
- Dozmorov, I. and Centola, M. (2003) An associative analysis of gene expression array data. *Bioinformatics*, **19**, 204–211.
- Dubois, M., Gilles, K.A., Hamilton, J.K., Rebers, P.A. and Smith, F. (1956) Colorimetric method for determination of sugars and related substances. *Anal. Chem.* **28**, 350–356.
- Fukushima, R.S. and Hatfield, R.D. (2004) Comparison of the acetyl bromide spectrophotometric method with other analytical lignin methods for determining lignin concentration in forage samples. *J. Agric. Food. Chem.* **52**, 3713–3720.
- Genty, B., Briantais, J.M. and Baker, N.R. (1989) The relationship between the quantum yield of photosynthetic electron transport and quenching of chlorophyll fluorescence. *Biochim. Biophys. Acta*, **990**, 87–92.
- Hatfield, R.D., Ralph, J. and Grabber, J.H. (1999) Cell wall structural foundations: molecular basis for improving forage digestibilities. *Crop Sci.* **39**, 27–37.
- Hélène, B., Olivier, R., Christelle, R., Michel, P., Claude, D. and Christophe, B. (2008) Analytical methodologies for quantification of ferulic acid and its oligomers. *J. Sci. Food Agric.* **88**, 1494–1511.
- Irizarry, R.A., Bolstad, B.M., Collin, F., Cope, L.M., Hobbs, B. and Speed, T.P. (2003) Summaries of Affymetrix GeneChip probe level data. *Nucleic Acids Res.* **31**, e15.
- Iwase, A., Hiden, A., Watanabe, K., Mitsuda, N. and Ohme-Takagi, M. (2009) A chimeric NST repressor has the potential to improve glucose productivity from plant cell walls. *J. Biotech.* **42**, 279–284.
- Jones, L., Milne, J.L., Ashford, D.A. and McQueen-Mason, S.J. (2003) Cell wall arabinan is essential for guard cell function. *Proc. Natl Acad. Sci. USA*, **100**, 11783–11788.
- Jones, L., Milne, J.L., Ashford, D.A., McCann, M.C. and McQueen-Mason, S.J. (2005) A conserved functional role of pectic polymers in stomatal guard cells from a range of plant species. *Planta*, **221**, 255–264.
- Keegstra, K. and Walton, J. (2006) Plant science. Beta-glucans – brewer's bane, dietician's delight. *Science*, **311**, 1872–1873.
- Kim, S.J., Kim, M.R., Bedgar, D.L., Moinuddin, S.G., Cardenas, C.L., Davin, L.B., Kang, C. and Lewis, N.G. (2004) Functional reclassification of the putative cinnamyl alcohol dehydrogenase multigene family in Arabidopsis. *Proc. Natl Acad. Sci. USA*, **101**, 1455–1460.
- Kowalska, I., Stochmal, A., Kapusta, I., Janda, B., Pizza, C., Piacente, S. and Oleszek, W. (2007) Flavonoids from barrel medic (*Medicago truncatula*) aerial parts. *J. Agric. Food. Chem.* **55**, 2645–2652.
- Lapierre, C., Monties, B. and Rolando, C. (1985) Thioacidolysis of lignin: comparison with acidolysis. *J. Wood Chem. Technol.* **5**, 277–292.
- Leek, J.T., Monsen, E., Dabney, A.R. and Storey, J.D. (2006) EDGE: extraction and analysis of differential gene expression. *Bioinformatics*, **22**, 507–508.
- Li, C. and Wong, W.H. (2001) Model-based analysis of oligonucleotide arrays: expression index computation and outlier detection. *Proc. Natl Acad. Sci. USA*, **98**, 31–36.
- Liepman, A.H., Wilkerson, C.G. and Keegstra, K. (2005) Expression of cellulose synthase-like (Csl) genes in insect cells reveals that CslA family members encode mannan synthases. *Proc. Natl Acad. Sci. USA*, **102**, 2221–2226.

- Mitsuda, N. and Ohme-Takagi, M. (2008) NAC transcription factors NST1 and NST3 regulate pod shattering in a partially redundant manner by promoting secondary wall formation after the establishment of tissue identity. *Plant J.* **56**, 768–778.
- Mitsuda, N., Seki, M., Shinozaki, K.M. and Ohme-Takagi, M. (2005) The NAC transcription factors NST1 and NST2 of Arabidopsis regulate secondary wall thickenings and are required for anther dehiscence. *Plant Cell*, **17**, 2993–3006.
- Mitsuda, N., Iwase, A., Yamamoto, H., Yoshida, M., Seki, M., Shinozaki, K. and Ohme-Takagi, M. (2007) NAC transcription factors, NST1 and NST3, are key regulators of the formation of secondary walls in woody tissues of Arabidopsis. *Plant Cell*, **19**, 270–280.
- Nakashima, J., Chen, F., Jackson, L., Shadle, G. and Dixon, R.A. (2008) Multi-site genetic modification of monolignol biosynthesis in alfalfa (*Medicago sativa*): effects on lignin composition in specific cell types. *New Phytol.* **179**, 738–750.
- Pfaffl, M.W. (2001) A new mathematical model for relative quantification in real-time RT-PCR. *Nucleic Acids Res.* **29**, e45.
- Ram, M.S., Dowell, F.E. and Seitz, L.M. (2003) FT-Raman spectra of unsoaked and NaOH-soaked wheat kernels, bran, and ferulic acid. *Cereal Chem.* **80**, 188–192.
- Ramakers, C., Ruijter, J.M., Deprez, R.H. and Moorman, A.F. (2003) Assumption-free analysis of quantitative real-time polymerase chain reaction (PCR) data. *Neurosci. Lett.* **339**, 62–66.
- Reddy, M.S.S., Chen, F., Shadle, G.L., Jackson, L., Aljoe, H. and Dixon, R.A. (2005) Targeted down-regulation of cytochrome P450 enzymes for forage quality improvement in alfalfa (*Medicago sativa* L.). *Proc. Natl Acad. Sci. USA*, **102**, 16573–16578.
- Shadle, G., Chen, F., Reddy, M.S.S., Jackson, L., Nakashima, J. and Dixon, R.A. (2007) Down-regulation of hydroxycinnamoyl CoA: shikimate hydroxycinnamoyl transferase in transgenic alfalfa affects lignification, development and forage quality. *Phytochemistry*, **68**, 1521–1529.
- Shen, H., Yin, Y., Chen, F., Xu, Y. and Dixon, R.A. (2009) A bioinformatic analysis of NAC genes for plant cell wall development in relation to lignocellulosic bioenergy production. *Bioenergy Res.* **2**, 217–232.
- Sibout, R., Eudes, A., Mouille, G., Pollet, B., Lapierre, C., Jouanin, L. and Seguin, A. (2005) CINNAMYL ALCOHOL DEHYDROGENASE-C and -D are the primary genes involved in lignin biosynthesis in the floral stem of Arabidopsis. *Plant Cell*, **17**, 2059–2076.
- Somerville, C. (2006) Cellulose synthesis in higher plants. *Annu. Rev. Cell Dev. Biol.* **22**, 53–78.
- Somerville, C. (2007) Biofuels. *Curr. Biol.* **17**, R115–R119.
- Storey, J.D. and Tibshirani, R. (2003) Statistical significance for genome-wide studies. *Proc. Natl Acad. Sci. USA*, **100**, 9440–9445.
- Tadege, M., Ratet, P. and Mysore, K.S. (2005) Insertional mutagenesis: a Swiss Army knife for functional genomics of *Medicago truncatula*. *Trends Plant Sci.* **10**, 229–235.
- Tadege, M., Wen, J., He, J. et al. (2008) Large-scale insertional mutagenesis using the Tnt1 retrotransposon in the model legume *Medicago truncatula*. *Plant J.* **54**, 335–347.
- Tanaka, K., Murata, K., Yamazaki, M., Onosato, K., Miya, O.A. and Hirochika, H. (2003) Three distinct rice cellulose synthase catalytic subunit genes required for cellulose synthesis in the secondary wall. *Plant Physiol.* **133**, 73–83.
- Town, C.D. (2006) Annotating the genome of *Medicago truncatula*. *Curr. Opin. Plant Biol.* **9**, 122–127.
- Turner, S.R., Taylor, N. and Jones, L. (2001) Mutations of the secondary cell wall. *Plant Mol. Biol.* **47**, 209–219.
- Yang, S.H., Xu, W.W., Tesfaye, M., Lamb, J.F.S., Jung, H.G., Samac, D.A., Vance, C.P. and Gronwald, J.W. (2009) Alfalfa biomass germplasm: SFP detection and transcriptome analysis. In *XVII Plant and Animal Genome Conference San Diego*, Abstract W167.
- Young, N.D. and Udvardi, M. (2009) Translating *Medicago truncatula* genomics to crop legumes. *Curr. Opin. Plant Biol.* **12**, 193–201.
- Zeng, Y., Saar, B.G., Friedrich, M.G., Chen, F., Liu, Y.-S., Dixon, R.A., Himmel, M.E., Xie, X.S. and Shi-You Ding, S.-Y. (2010) Imaging lignin-down-regulated alfalfa using Coherent Anti-Stokes Raman Scattering Microscopy. *Bioenergy Res.* **3**, in press.
- Zhong, R., Richardson, E.A. and Ye, Z.H. (2007) Two NAC domain transcription factors, SND1 and NST1, function redundantly in regulation of secondary wall synthesis in fibers of Arabidopsis. *Planta*, **225**, 1603–1611.
- Zhong, R., Lee, C., Zhou, J., McCarthy, R.L. and Ye, Z.H. (2008) A battery of transcription factors involved in the regulation of secondary cell wall biosynthesis in Arabidopsis. *Plant Cell*, **20**, 2763–2782.
- Zhou, J., Lee, C., Zhong, R. and Ye, Z.H. (2009) MYB58 and MYB63 are transcriptional activators of the lignin biosynthetic pathway during secondary cell wall formation in Arabidopsis. *Plant Cell*, **21**, 248–266.